Dynamic Sub-THz Radio Channel Emulation

Principle, Challenges, and Experimental Validation

Zhang, Fengchun; Bengtson, Mikkel Filt; Kyosti, Pekka ; Kyröläinen, Jukka; Fan, Wei

Published in:
I E E E Wireless Communications Magazine

DOI (link to publication from Publisher):
10.1109/MWC.001.2300286

Publication date:
2024

Document Version
Accepted author manuscript, peer reviewed version

Dynamic Sub-THz Radio Channel Emulation: Principle, Challenges, and Experimental Validation

Fengchun Zhang, Mikkel Filt Bengtson, Pekka Kyösti, Jukka Kyröläinen, and Wei Fan, *Senior member, IEEE*

***Abstract*—Sub-terahertz (Sub-THz) technology, as one of the key candidates for the six generation (6G) systems, has attracted increasing attention from academia and industry, due to its promise to unleash vast amounts of new frequency spectrum. Sub-THz system designs pose unique and more challenging circumstances compared to traditional communication systems. These challenges arise from the demanding propagation conditions, limited availability of commercial radio frequency (RF) components, the need for high-gain and beam-steerable antennas that are highly integrated at both ends of the communication link, short-range communication scenarios, and the requirement for extreme data rates. Therefore, it is crucial to assess the performance of radio devices in realistic propagation channels in sub-THz communication systems. In this work, we present the concept, challenges, and enabling solutions for achieving sub-THz radio channel emulation. Moreover, we experimentally demonstrated the reconstruction of the measured propagation channels at 140 GHz with a commercial radio channel emulator in the laboratory. The developed dynamic fading channel replay concept and experimental validation procedure allows initial tests of future sub-THz communication devices.**

***Index Terms*—Sub-THz, 6G, channel emulation, radio propagation, channel sounding and replay.**

I. Introduction

IT is expected that 6G connectivity will operate across a broad spectrum of frequency bands, catering to a diverse range of 6G user cases. The sub-THz frequency range has the potential to provide wide blocks of lightly or even untapped spectrum, making it highly attractive for 6G user cases that demand ultra-high data rate transmission with exceptionally low latencies, e.g., direct device-to-device communication, extreme gaming and fully integrated cyber physical world [1], [2].

Radio channel modeling describes how electromagnetic signals propagate and interact with the environment between a transmitter (Tx) and a receiver (Rx), which is vital in design, development and performance testing of wireless communications systems. Significant efforts have been made in the academia and industry to investigate radio channels at sub-THz, e.g. channel sounder development [1], ray tracing (RT) simulation [2], and standardization efforts. Compared to legacy frequency bands, radio signal transmission at sub-THz faces several new challenges. As the radio frequency goes up, a few trends in the propagation channel have been reported in the state-of-the-art works. Free-space path loss will increase according to Friis' formula. Sub-THz channels will become highly sparse and specular, which means signal transmission mainly relies on a few dominant propagation paths originated from line-of-sight (LOS) and reflection transmissions. Moreover, sub-THz channels are susceptible to blockage and motion in the environment, making it highly dynamic. To achieve the high date-rate and reliable transmission promised by the large system bandwidth at sub-THz, the signal-to-noise ratio (SNR) should be maintained high. The Tx power and Rx sensitivity are unfortunately constrained due to current technology. To address the high propagation loss and maintain the signal link quality, it is essential for sub-THz systems to incorporate high gain and beam-steerable antenna systems at both the Tx and Rx sides, to track and align the dominant propagation paths in the channel. Owing to the small wavelength in sub-THz frequency bands, sub-THz systems of the same physical aperture can in principle accommodate several orders of magnitude more elements than sub-6 GHz systems, making it possible to provide sufficient signal power in the communication link. Beam-steerable antennas are also essential for the beam management in real-world dynamic deployment scenarios.

To make sub-THz communication a reality, one essential step is to validate 6G radios under realistic RF propagation channel conditions. Moreover, it would be desirable that the realistic sub-THz channels can be emulated in laboratory conditions for performance testing of sub-THz radios. A radio channel emulator (CE) has been widely employed for air interface testing [3]–[8]. This allows for achieving virtual field-testing purposes, which is essential to test sub-THz radios under various representative operating scenarios in a controllable and repeatable manner. There is a strong need from industry for a standard and cost-effective testing solution to pave the way for the success of rollout of sub-THz enabled 6G deployment.

However, there are still many gaps and challenges to overcome in order to achieve sub-THz channel emulation. Most commercial CEs that are developed for sub-6 GHz applications [3], can support mmWave frequency bands by utilizing external frequency up-converters [4], [5]. Though the supported system bandwidth of a single channel unit is rather limited, e.g., up to 160 MHz in [4], a bandwidth enhancement scheme such as a band-stitching concept [5] can be adopted to extend the bandwidth. For example CE bandwidths up to 500 MHz in [4] and 960 MHz in [6] were experimentally demonstrated. In addition, the CE resource, i.e., the number of

F. Zhang and M. Bengtson are with the Department of Electronic Systems, Aalborg University, Denmark.

P. Kyösti and J. Kyröläinen are with Keysight Technologies, Oulu, Finland.

Wei Fan (corresponding author, weifan@seu.edu.cn) is with Southeast University, China.

P. Kyösti and W. Fan are also with center for wireless communication (CWC), Oulu University, Finland.

delay taps, is inherently limited due to the computationally intensive nature of implementing fading channels in a digital CE [7]. As explained, beam-steering and beam alignment towards dominant propagation paths in highly dynamic propagation environment is of critical importance in sub-THz radios, and must be evaluated by appropriate emulation models. Last but not least, sub-THz radios will be highly integrated and packed with thousands of antennas, making traditional cabled testing which requires a cable connection to a CE, obsolete.

In this work, the focus is on the concept, challenges, and enabling solutions for achieving dynamic sub-THz radio channel emulation. More specifically, our key contributions are listed as below:

- We identify the key requirements for sub-THz channel emulation, covering aspects related to carrier frequency, system bandwidth, channel emulator resource, channel models, and interface between testing instruments and sub-THz radios.
- We discuss the enabling solutions applicable for the sub-THz radios, including the frequency extension scheme for down/up-converting signals from/to sub-THz bands, the band-stitching concept to enhance the emulation bandwidth, the tap resource optimization scheme to reduce required CE resource, the site-specific dynamic channel modeling considering blockage and channel transition, and the wireless cable concept for achieving over-the-air connection.
- We experimentally demonstrate fading channel replay for measured sub-THz channels using a commercial CE platform. Dynamic channels with a sub-THz radio capable of beam-steering and alignment scheme were emulated and validated in the experimental setup.

II. Sub-THz channel emulation

A. Basic principle for digital CE

A CE is dedicated testing equipment (hardware) designed to emulate the propagation of radio waves. The channel simulator (e.g., geometry-based stochastic channel, 3GPP 38.901) or RT (typically software) is a simulation platform for simulating propagation channels and generating associated channel impulse responses (CIRs). Channel emulation physically replicates radio channels in a laboratory environment to mimic real-world conditions. The CIRs loaded in the CE (implemented with the finite impulse response (FIR) in the baseband) can be generated through standard channel simulator, RT simulation or channel measurements, among others. The CE provides the capability to create reproducible and controllable propagation conditions for radio performance verification, which is often challenging to achieve through field testing.

An illustration of the digital CE (highlighted by the black box) is shown in Fig. 1. In this diagram, ADC and DAC denote the analog-to-digital converter and digital-to-analog converter, respectively. f_n^{IF} and h_n^{BB} denote the carrier frequency setting and CIR in the baseband for the n-th sub-channel, respectively. In operation, the RF signal transmitted by the Tx is down-converted and digitized into a stream of in-phase and quadrature (IQ) samples. These samples are then digitally processed, specifically convolved, with the time-variant multipath channel profiles in real-time using digital signal processing (DSP) units. The processed signal is then upconverted in the CE and coupled into the Rx. Notably, for sub-THz frequency bands, where there are no reserved antenna ports for cable access, probe antennas are used to send/receive testing signals over-the-air to the CE. Digital CEs based on tapped delay line (TDL) structure are popular, owing to their capability of implementing flexible and standard multipath channels based on FIR filter structure. Note that a multiple-input multiple output (MIMO) CE with N input ports and M output ports would necessitate $N \times M$ fading channels, while bi-directional emulation would require doubling the fading channel resources.

B. Challenges and enabling solutions

1) Extension to sub-THz carrier frequency band: Current commercial digital CEs, initially designed for sub-6GHz applications, can expand to cover mmWave frequency bands using mixer to up-convert and down-convert the signal frequency [4]. For broader frequency range, frequency extension modules, commonly used in sub-THz channel sounders [1], are employed as shown in Fig. 1. The sub-THz carrier frequency for the RF chain can be flexibly design via properly setting the local oscillator (LO) frequency, the intermediate frequency (IF) in the CE, and the multiplier in the frequency extender. CIRs implemented in the sub-6GHz CE can be directly used for the sub-THz channel emulation, with adjustments to the absolute Doppler frequency as explained in [4].

2) Bandwidth enhancement scheme: An enormous bandwidth will be utilized at sub-THz. However, current commercial CEs, designed for testing of existing systems like 4G LTE, 5G new radio (NR) and WiFi, have limited system bandwidth due to expensive ADCs and DACs. A software defined radio platform-enabled mmWave CE in [8] achieved a 3 GHz instantaneous bandwidth. The state-of-the-art works [5], [6] demonstrated the effectiveness of the band-stitching scheme. This scheme combines multiple digital channels operating at different IFs (covering the intended wide frequency band), to create a single, broader digital channel, effectively enhancing system bandwidth. It leverages a power splitter, multiple fading channel units, and a power combiner within the CE, as illustrated in Fig. 1 with N sub-channels. It was demonstrated that homogeneous sub-band channels (i.e. with phase and amplitude calibrated) are essential to ensure the quality of the stitched wideband digital channel [4].

3) CE resource optimization: For commercial digital CEs, the delay tap resource is essentially limited. When more fading channels are required, such as for MIMO or bi-directional channel emulation, the number of delay taps per channel is reduced due to computational limitations in the DSP units. Additionally, delays in commercial CEs are discrete, determined by the CE's sampling frequency. However, practical propagation channels may have arbitrary numbers of delay taps and locations. Therefore, optimizing the tap resource of the CE, including the number of delay taps, their delay locations, and the assigned complex coefficients, is crucial.

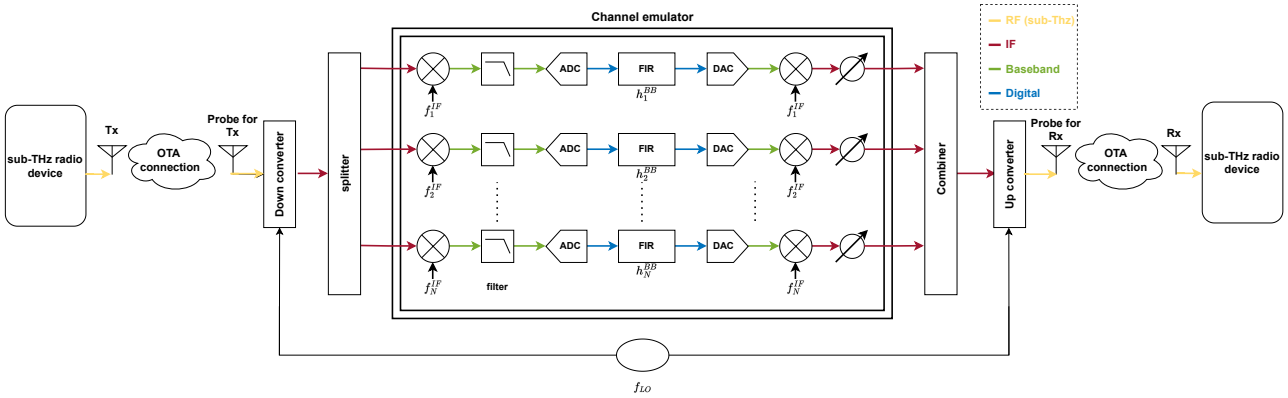

Fig. 1. Diagram of a sub-THz CE for single-input single-output (SISO) transmission, with the band stitching scheme using N sub-channels.

This optimization ensures that the CE can accurately reproduce the target channel profiles to the greatest extent possible.

One widely adopted method, as proposed in [9], is the rounding delay method. This approach aligns the delays of dominant multipaths in the target channels with the closest tap delay grid of the CE. Although simple, its performance is limited by distortion or artifacts caused by rounding errors, especially when the CE has poor delay resolution due to limited sampling bandwidth. In contrast, the fractional delay filter method provides a superior alternative. This method optimizes delay taps and complex coefficients to match the target channel frequency response (CFR), resulting in improved performance and fewer artifacts. In [10], a solution based on orthogonal matching pursuit algorithm was introduced. This solution sequentially selects dominant delay taps and optimizes tap coefficients by exploiting the delay sparsity in propagation channels.

4) Over-the-air interface connection: In traditional cabled setups, testing signals are routed from testing instrument ports (e.g., CE output or input interfaces) to the device under test (DUT) antenna ports through RF coaxial cables, bypassing built-in DUT antennas. This solution has been dominant for sub-6 GHz radios where testing through reserved antenna connectors is feasible. However, for sub-THz radios, characterized by compact and integrated designs, the use of highly lossy, expensive, and fragile sub-THz connectors is impractical. As a result, over-the-air radiated testing, employing sub-THz built-in antennas as direct interfaces for signal transmission and reception, will be the dominant method.

Sub-THz radio with analog beamformer structure, sharing a common RF source among multiple antenna elements, will be dominant at least in its early release. To ensure distortion-free signal transmission to the respective sub-THz DUT antenna ports, the transfer coefficient matrix between the probe antenna (connected to the testing instrument) and the sub-THz radio antenna needs calibration. For single-input single-output (SISO) transmission with only a line-of-sight (LOS) path in the testing environment (e.g., an anechoic chamber), power calibration suffices. However, for MIMO transmission involving spatial, polarization, or beam domain techniques, careful calibration of the transfer matrix is essential [11].

5) Suitable radio channel models for sub-THz emulation: Geometry-based stochastic channel modeling, rooted in the concept of channel clusters (groups of unresolvable multi-path components), has been widely adopted in 4G and 5G standardization. Clustering simplifies modeling for channels with rich multipath components, which is suitable for 4G and 5G radios due to their limited delay and spatial resolutions. However, it may be less suitable for sub-THz radios. Sub-THz propagation channels are sparse and specular, with few dominant paths. Sub-THz radios use highly directional antennas, further spatially filtering channels, resulting in even sparser characteristics. In addition, sub-THz systems offer high delay and spatial resolution due to vast bandwidth and electrical apertures.

Recent channel measurements using both frequency domain [1] and time-domain channel sounders [12] have focused on sub-THz propagation channels, primarily in static environments due to slow mechanical positioning and orientation system. Real-time sub-THz channel sounders are complex and costly, making dynamic spatial channel measurements an open challenge. An alternative approach is RT simulation, which utilizes geometric optics principles to model the propagation of electromagnetic waves as they interact with objects, surfaces and materials in complex environments. It allows simulation and analysis of different scenarios with various configurations and environmental conditions, such as antenna placement, material properties, or the presence of obstacles. RT also offers flexibility for investigating dynamic channel characteristics by adjusting parameter settings. RT shows promise for modeling sub-THz propagation characteristics for 6G [2].

As discussed, high gain and beam-steerable antennas are crucial for maintaining consistent alignment with the dominant propagation path, ensuring optimal connectivity even as environments and transceiver positions change. Evaluating realistic sub-THz communication links requires considering dynamic channels resulting from the movement of communication ends and objects. Furthermore, adaptive beamforming at both communication links is essential for real-time steering towards the most dominant propagation path.

III. CE RESOURCE OPTIMIZATION FOR DYNAMIC CHANNELS

To demonstrate dynamic channel emulation capabilities, we simulate a scenario transitioning between non-LOS (NLOS) and LOS regions using RT simulation. Furthermore, we implemented band-stitching and CE resource optimization strategies to emulate wideband dynamic channels using practical CEs with limited bandwidth and tap resources.

A. Dynamic channel simulation

In the RT simulation, two omni-directional antennas with a gain of 0 dB and a half-power beam width (HPBW) of 30^o in the elevation were employed as the Tx and the Rx antenna, respectively. Both antennas were positioned 1.25 m above the ground. The simulation scenario is illustrated by Fig. 2 (a), where the Tx antenna remains fixed while the Rx antenna moves through 31 positions in 0.5 m increments, transitioning from NLOS to LOS and back to NLOS regions, as indicated by the blue arrow. The Rx locations are numbered from 1 to 31 as shown in Fig. 2 (a). For each location, we selected the 100 strongest paths from the RT simulation, which served as the target fading channels. The simulations were performed using the Wireless InSite 3D wireless prediction software. Note that beam-steering and tracking were not implemented in the numerical simulations. Additionally, the simulation frequency in the RT was set to 3.5 GHz. All the algorithms for the CE were implemented in the baseband, and therefore its performance is not related to the carrier frequency.

B. CE setting

In the channel emulation simulation, we set the carrier frequency to the D-band at 140 GHz. We form a wideband CE with a bandwidth of 500 MHz as an example, using 4 sub-bands with each covering a bandwidth of 135 MHz. The measured system frequency response for each sub-channel of 135 MHz in the CE bypass mode [4] was adopted in the optimization. In the simulation, we adopt three different numbers of taps in the CE, namely 24, 12, and 6, to emulate the fading channels across the targeted 500 MHz bandwidth. For each sub-band, we implement tap selection and coefficient optimization strategy method [10]. In theory, using 4 sub-bands, each with a 135 MHz bandwidth, we can create a single virtual digital channel with a total bandwidth of $4 \times 135 = 540$ MHz. However, this configuration assumes filters with ideal rectangular frequency responses, which are non-causal and have infinite delay, making them impractical. In practice, we employ a raised cosine filter for each sub-band. Careful design of the individual center frequencies and calibration of these sub-bands ensures appropriate overlapping among adjacent sub-bands, resulting in an approximately flat response over the stitched wide band [11].

C. Simulation results

The CIRs of the target dynamic channels over the trajectory (i.e. 31 locations) are plotted in Fig. 2 (b) as the reference for evaluating the quality of the emulated channels. It can be observed that the CIR gradually changes as the Rx moves from the location 1 to 31. This variation is due to the channel conditions transitioning from NLOS (at locations 1-7) to LOS (at locations 8-17), and then back to NLOS (at locations 18-31). It is noticeable that the NLOS conditions exhibit lower power and larger delay compared to the LOS conditions for the first arrival path at each Rx location, as expected.

The emulated CIRs over the trajectory are depicted in Fig. 2(c)-(e) with 24, 12, and 6 taps, respectively. The power levels of the target channels (b) and emulated channels (c)-(e) share the same dynamic range, represented by a single color bar for (c)-(e). While dominant paths show a close match between emulated and target CIRs, deviations are noticeable, especially for weaker paths when tap count is reduced. These discrepancies highlight that emulated channels are not identical to the target ones. These discrepancies result from limitations in commercial CEs, including system bandwidth constrains, distortion from band stitching, discrete delays, and a restricted number of delay taps due to DSP computational constraints. Note that commercial CEs generally performs channel emulation in the time domain, not in the frequency domain to minimize insertion delay and extra latency that would occur when transforming between frequency and time domains. Therefore, optimizing the CE's delay taps, their locations, and complex coefficients is essential. This optimization focuses on accurately representing dominant paths while compromising in emulating weaker paths, all within the constraints set by commercial CEs.

The simulation results demonstrate that even with a limited number of taps, the tap selection and tap coefficient optimization method in [10] can effectively emulate dynamic fading channels over a targeted wide band stitched together from multiple sub-bands. This is achieved through the implementation of sub-band calibration for band stitching and fading channel emulation within the digital channels of CEs.

IV. SUB-THZ CE EXPERIMENTAL MEASUREMENTS

Experimental measurements were conducted to validate the channel emulation concept in the sub-THz band. In these experiments, a commercial CE operating at sub-6 GHz was used to emulate fading channels over a wide bandwidth.

A. Experimental platform

In the experimental platform, we use a digital UE to emulate the target channels and measure the emulated channel profile using A VNA. Note that neither the CE nor the VNA inherently supports sub-THz frequency bands. Therefore, validating sub-THz channel emulation requires two sets of frequency extenders, one set for the CE and the other set for the VNA, for frequency up- and down-conversion. However, due to their high cost, we have only one set (i.e., one up- and one down-conversion units) available in the lab. Moreover, it is expected that frequency extenders do not affect signal characteristics too much and even if they did, the focus of this work is not in evaluation of up- and down-conversions. It is essential to mention that we did not implement any frequency extension to and from sub-THz during the measurements due to the lack

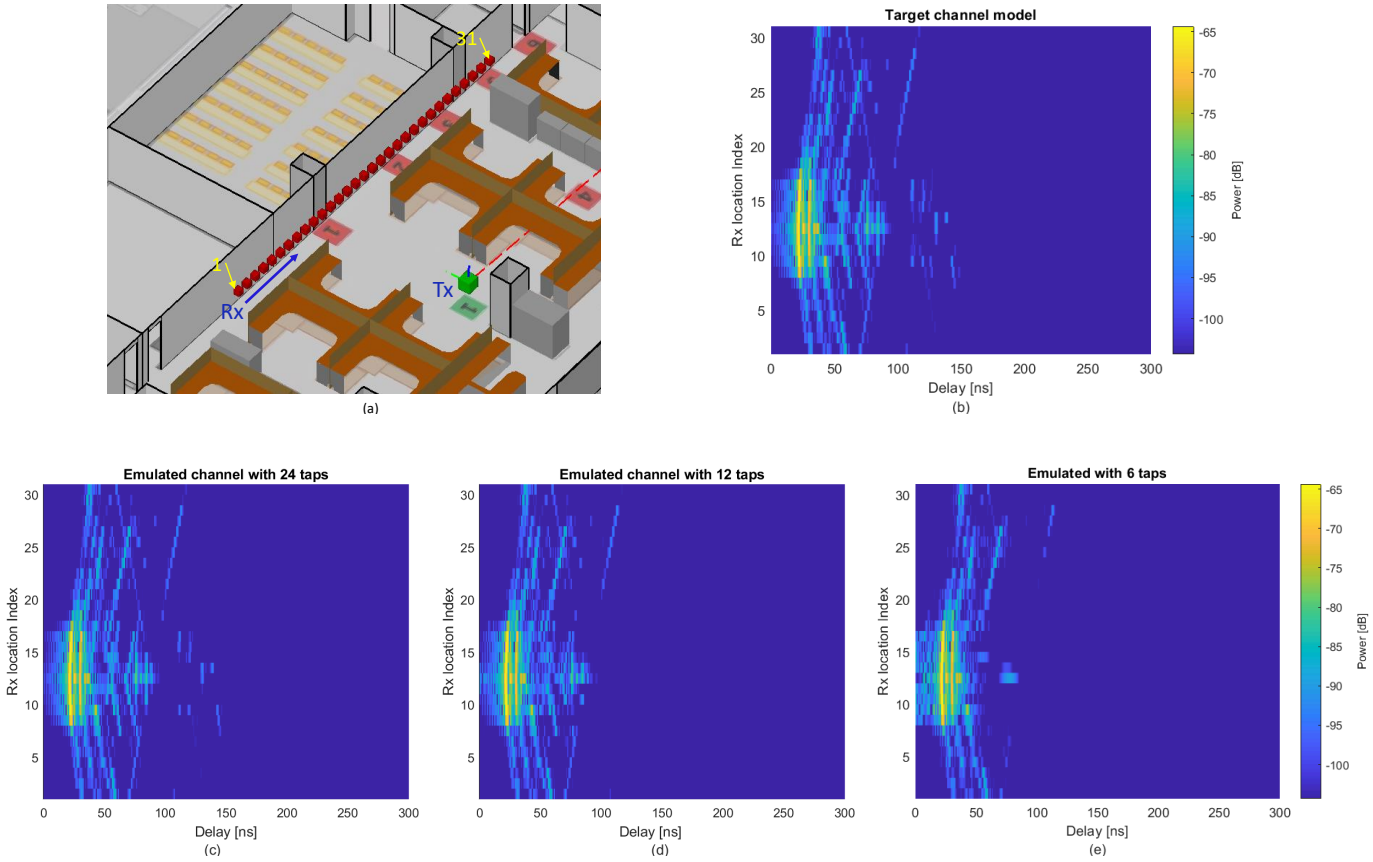

Fig. 2. Dynamic fading channel emulation: (a) RT simulation scenario, (b) the CIRs of the target channels over the trajectory, the CIRs of the emulated channel over the trajectory by using (c) 24 taps, (d) 12 taps, and (e) 6 taps, respectively.

of frequency extenders for both the CE and VNA. Instead, we measured or simulated the time-variant wideband channels at sub-THz bands and then emulated the sub-THz channels at sub-6 GHz to align with the supported frequency band of the CE. The baseband CIRs, implemented in the baseband FIR in the CE, are consistent with the replayed sub-THz channels. Frequency conversion introduces possible unwanted nonlinearities to the system, which are not part of the target propagation channel. Additionally, the CIR update rate for the dynamic channel should be scaled according to the target sub-THz and CE sub-6 GHz carrier frequency, as demonstrated in [4] for mmWave CEs.

A photo of the measurement setup is shown in Fig. 3, which composes the following components:

- a commercial Keysight Propsim FS16 was employed for emulating channels. The CE's carrier frequency was set to 2 GHz, and a bandwidth of 1.2 GHz was achieved through the discussed band-stitching concept.
- a Keysight VNA PNA-X was used to measure the channels emulated by the CE. The measurement was conducted with a center frequency of 2 GHz, a bandwidth of 1.4 GHz, and 1001 frequency points to fully capture the emulated CFRs.
- a control PC was utilized to configure and control the CE for emulating specific channels.

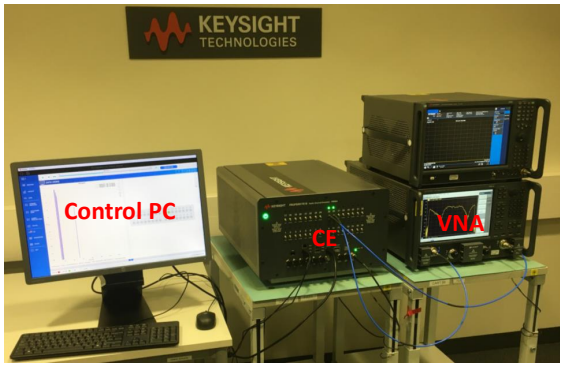

Fig. 3. The photo of the measurement setup.

B. Dynamic sub-THz channel models

Two types of dynamic channel models were considered in the validation of sub-THz channel emulation.

1) "blockage scenario": The "blockage scenario" involves static Tx and Rx locations and intentionally introduces a "human blocker" to emulate environment changes due to a moving object, as depicted in Fig. 4 (a) (LOS) and (b) (NLOS with LOS blocked by the human blocker). To model this scenario, we extend the original measurement based CIR using

RT simulation, assuming isotropic antennas at both ends. The channel sounding measurement spans 140-144 GHz, while the RT is simulated at 140 GHz as described in [13]. Blockage events occur when paths approach within 0.8 meters of the human blocker's center, moving at 1 m/s. The attenuation profile of the human blocker, obtained from measurements at 140 GHz within a 2 GHz bandwidth as elaborated in [14], is integrated into double directional data by scaling individual path gains with a time-variant attenuation factor. Beam-steering is implemented at both communication ends to track and align with the strongest path, ensuring link stability. This results in the identification of LOS and NLOS paths in Fig. 4 (a) and (b), respectively.

2) "Transition scenario": The "transition scenario" characterizes the channel changing when one of the link ends, either the Tx or the Rx, moves from the NLOS region to the LOS region while the environment remains static. Beamforming is implemented at both communication ends to track the most dominant propagation path. The main goal is to emulate the movement of the Tx/Rx within a propagation scenario, where the LOS conditions change.

Double directional sub-THz channel measurements, covering a frequency range from 110 to 170 GHz, were conducted in the corridor scenario at two Rx locations, one in the NLOS and the other one in the LOS location in [15], as indicated by the the blue and orange dots in 5(a), respectively. Based on measurement data, the double directional channels for the transitional locations between these two locations (indicated by the gray dots) were interpolated using RT simulation. The interpolation considered free space path loss, reflection loss for determining power level and delay based on ray traveling distances. The angles of arrival and departure were interpolated using the geometry of the identified rays. These transitional positions allowed for a more comprehensive analysis of signal behavior as the Rx antenna moved gradually from NLOS to LOS or vice versa. In the RT simulation, a total of 7 Rx locations were modeled with a separation distance of 0.35 m, spanning a length of 2.08 m. Three channel models were exported from the RT simulation, with the Rx antenna located at the left end (0 m), center (1.04 m) and right end (2.08 m), as highlighted in the Fig. 5 as an example.

C. Measurement results

1) "blockage scenario": In the "blockage scenario", the measured CIRs of the emulated channels are compared with the target channel models in Fig. 4 (c) for both "blocker" positions. In the figure, "Gain" represents the channel gain in dB, reflecting the amplitude of the CIR. "Model" corresponds to the CIRs obtained from the RT simulation, and "Measurement" denotes the CIRs of the channel emulated by the CE and measured with a VNA. In the RT simulation, the channel gains of the individual multiple paths are normalized so that the strongest path without the blockage effect has unity gain. Inside a CE, the path gains are further normalized to ensure the average sum gain equals unity. Therefore, the gains in the figure are represented as normalized values.

Comparing the channels at the two 'blocker' positions, we observe noticeable differences. In the NLOS case (position 2), there are fewer paths within the 40 dB dynamic range compared to the LOS case (position 1), and the paths in the NLOS case are less spread out. These differences can be primarily attributed to two factors: the blockage effect and the shift in the main beam direction of the Rx antenna towards the strongest NLOS path. In NLOS conditions, obstacles and environmental conditions cause the signal to deviate from a direct LOS path, resulting in multiple scattering and reflections.

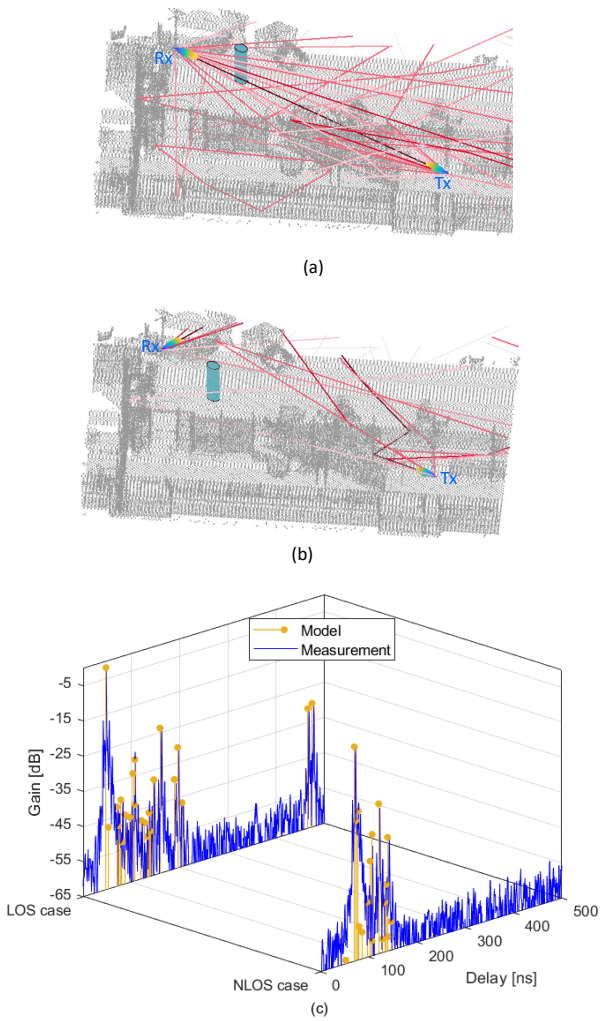

Fig. 4. "Blockage scenario": (a) the RT simulation scenario in the LOS case (with the blocker at position 1), (b) the RT simulation scenario in the NLOS case (with the blocker at position 2) and (c) measured and target CIRs for both cases.

When comparing the CIRs between the emulated channels and the target channels in Fig. 4 (c), a good alignment between the emulated and target channels can be observed for the dominant paths in both cases. Some noticeable delay deviations for certain paths can be seen, primarily resulting from the discrete delays with a resolution of 5 ns in the CE. The LOS path exhibits a delay of 47.1 ns, suggesting a distance of approximately 14.1 m between the Tx and the Rx. Some sidelobes appear around the peaks of the multipaths, which could be attributed to the windowing effect of the raised cosine filter in the CE.

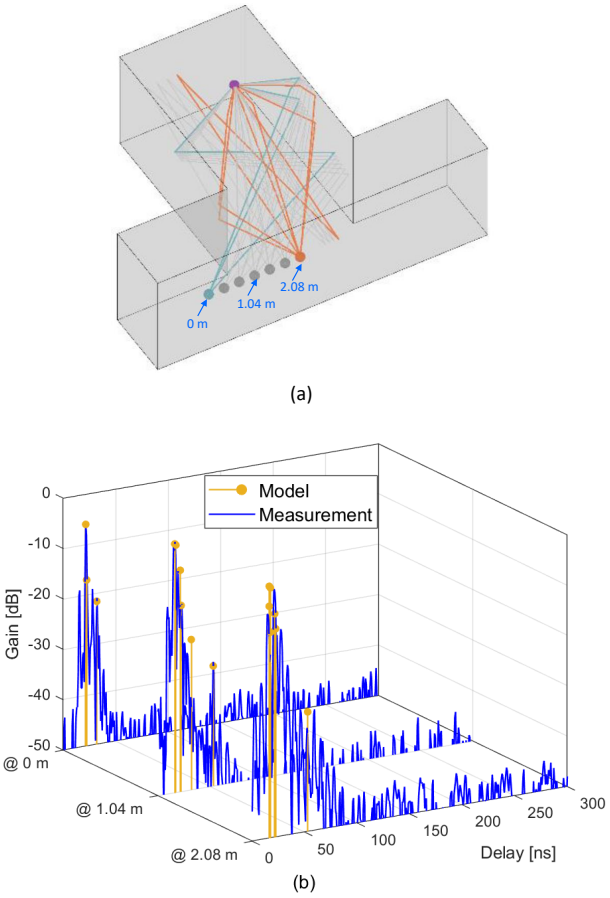

Fig. 5. "Transition scenario": (a) an illustration of the RT simulation scenario and (b) the measured CIRs at 0 m, 1.04 m and 2.08 m.

2) "transition scenario": In the "transition scenario", we compare the measured results with the target models for three different locations, as illustrated in 5 (b). An excellent alignment between the measured emulated channel and the target channel can be observed for all locations. As the Rx antenna moves from the NLOS condition (positioned at 0 m) to the LOS conditions (positioned at 1.04 m and 2.08 m), a few changes in the channel characteristics can be observed. Specifically, the gain of the strongest path in the CIR increases as the direct LOS path becomes dominant in the LOS conditions.

The overall observations indicate that the emulated channels effectively capture the characteristics of the target channels for both the blockage and transition scenarios. The measured results align well with the expected behaviors in real-world wireless communication scenarios, highlighting the capabilities of the emulated channel models in accurately replicating wireless propagation conditions.

V. Conclusion

Evaluating the performance of wireless systems in realistic propagation channels is crucial. In this work, we address the requirements, challenges, and solutions for achieving dynamic sub-THz channel emulation in beam-steerable sub-THz radios. We also explore concepts such as band stitching and CE tap resource optimization to meet the wideband system bandwidth and limited CE tap resource requirements. We conducted an experiment using a commercial CE to emulate sub-THz channel models with a 1.4 GHz bandwidth, focusing on scenarios involving indoor human blockage and transitions in beam-steerable sub-THz radios. The results of our experiment demonstrated excellent emulation accuracy.

Acknowledgment

The authors thank Mr. Zhiqiang Yuan for technical discussion. This work was supported in part by the start-up Research Fund of Southeast University, China, under Project RF1028623309; and in part by the European Partnership on Metrology Project MEWS funded by the European Partnership on Metrology (under Grant 21NRM03). This publication is based upon work from COST Action INTERACT, CA20120.

References

[1] A. Ghosh and M. Kim, "THz channel sounding and modeling techniques: An overview," *IEEE Access*, 2023.

[2] C. Han, Y. Wang, Y. Li, Y. Chen, N. A. Abbasi, T. Kürner, and A. F. Molisch, "Terahertz wireless channels: A holistic survey on measurement, modeling, and analysis," *IEEE Communications Surveys & Tutorials*, vol. 24, no. 3, pp. 1670–1707, 2022.

[3] "F8800b propsim F64 radio channel emulator," *Data Sheet, Keysight Technol., USA, 2022. [Online]. Available: https://www.keysight.com/ie/en/assets/3122-2164/data-sheets/F8800B-PROPSIM-F64-Radio-Channel-Emulator.pdf*.

[4] W. Fan, P. Kyösti, L. Hentilä, and G. F. Pedersen, "A flexible millimeter-wave radio channel emulator design with experimental validations," *IEEE Transactions on Antennas and Propagation*, vol. 66, no. 11, pp. 6446–6451, 2018.

[5] Y. Ji and W. Fan, "Enabling high-fidelity ultra-wideband radio channel emulation: Band-stitching and digital predistortion concepts," *IEEE Open Journal of Antennas and Propagation*, vol. 3, pp. 932–939, 2022.

[6] J. Cao, F. Tila, and A. Nix, "Design and implementation of a wideband channel emulation platform for 5G mmWave vehicular communication," *IET Communications*, vol. 14, no. 14, pp. 2369–2376, 2020.

[7] J. Sozanski and T. Grosch, "Radio frequency multipath channel emulation system and method," Sep. 8 2015, US Patent 9,130,667.

[8] "Real-time massive MIMO channel emulation." NYU WIRELESS, Tech. Rep. [Online]. Available: http://wireless.engineering.nyu.edu/realtime-massive-mimo-channel-emulatio.

[9] S. Schmidt, "Measuring device and method with efficient channel simulation," Jun. 9 2020, US Patent 10,680,723.

[10] A. W. Mbugua, Y. Chen, L. Raschkowski, Y. Ji, M. Gharba, and W. Fan, "Efficient pre-processing of site-specific radio channels for virtual drive testing in hardware emulators," *IEEE Transactions on Aerospace and Electronic Systems*, 2022.

[11] W. Fan, L. Hentilä, and P. Kyösti, "Spatial fading channel emulation for over-the-air testing of millimeter-wave radios: concepts and experimental validations," *Frontiers of Information Technology & Electronic Engineering*, vol. 22, no. 4, pp. 548–559, 2021.

[12] S. Rey, J. M. Eckhardt, B. Peng, K. Guan, and T. Kürner, "Channel sounding techniques for applications in THz communications: A first correlation based channel sounder for ultra-wideband dynamic channel measurements at 300 GHz," in *2017 9th international congress on ultra modern telecommunications and control systems and workshops (ICUMT)*. IEEE, 2017, pp. 449–453.

[13] M. F. De Guzman, P. Koivumäki, and K. Haneda, "Double-directional multipath data at 140 GHz derived from measurement-based ray-launcher," in *2022 IEEE 95th Vehicular Technology Conference:(VTC2022-Spring)*. IEEE, 2022, pp. 1–6.

[14] P. Zhang, P. Kyösti, M. Bengtson, V. Hovinen, K. Nevala, J. Kokkoniemi, and A. Pärssinen, "Measurement-based characterization of D-band human body shadowing," in *2023 17th European Conference on Antennas and Propagation (EuCAP)*. IEEE, 2023, pp. 1–5.

[15] J. Kokkoniemi, V. Hovinen, K. Nevala, and M. Juntti, "Initial results on D band channel measurements in LOS and NLOS office corridor environment," in *2022 16th European Conference on Antennas and Propagation (EuCAP)*. IEEE, 2022, pp. 1–5.